International Journal of Scientific Research in Physics and Applied Sciences **Research Paper**
Vol.7, Issue.3, pp.94-108, June (2019) **E-ISSN:** 2348-3423
DOI: https://doi.org/10.26438/ijsrpas/v7i3.94108

Vibrational Spectral Analysis (Ft-Ir And Ft-Raman) Andnlo, Homo Lumo And Mep Analysis Of 4, 4 Isopropylidenebis 2,6 Dichlorophenol

S. Saravanan[1], G. Kanagan[2], G. Satheeshkumar[3], S.Pari[4], R. Sambasivam[5]

[1,2,3,4]Department of Physics, National College (Autonomous), Triuchirappalli -620 001
[5]Department of Physics, Urumu Dhanalakshmi College, Triuchirappalli-620 019

Available online at: www.isroset.org

Received: 08/May/2019, Accepted: 09/Jun/2019, Online: 30/Jun/2019

***Abstract*-** The experimental and theoretical study on the structures and vibrations of 4,4-ISOPROPYLIDENE BIS 2,6-DICHLOROPHENOL (abbreviated as 4IBD) are presented. The FT-IR and FT-Raman spectra of the title compound have been recorded in the region 4000−400 cm^{-1} and 3500−100 cm^{-1} respectively. The molecular structures, vibrational wavenumbers, infrared intensities and Raman activities were calculated using DFT (B3LYP) method with 6-31+G (d) basis set. The most stable conformer of 4IBD) is identified from the computational results. HOMO and LUMO energies were determined by time-dependent TD-DFT approach. Molecular electrostatic potential map also analysis by this present compound, respectively.

***Keywords*-** 4, 4-ISOPROPYLIDENE BIS 2,6-DICHLOROPHENOL**,** Mulliken analysis, FT-IR,FT-Raman, HOMO and LUMO,extra

I. INTRODUCTION

The electro negative atom such as halogen attached to the (dichirophenal) phenol in a highly reactive the dichirophenal. The 4, 4′-isopropylitenepis (2,6-dichirophenol) phenal is a white crystalline powder with molecular formula ($C_{15}H_{12}Cl_4O_2$).The vibration spectroscopic using DFT methods have reported on methyl phenol. Therefore the present investigation was undertaken study the vibration of FT-IR, FT-Raman spectra of the molecule completely and to identify the vibrations normal modes with grater wave number accuracy. Predication of vibration frequency of polyatomic molecules by quantum chemical calculation has become very popular because of accurate and consistent description of the experimental data. 4pmp was investigated by using B3LYP calculation with 6-31+G (d) and 6-311++G (d, p) basis sets.

1. EXPERIMENTAL DETAILS

The sample IPDP in the solid form was provided by the Lancaster Chemical Company (UK) with a purity of greater than 98% and it was used as such without further purification. The FT-Raman spectrum of IPDP was recorded using 1064 nm line of Nd:YAG laser as excitation wavelength in the region 3500-100 cm^{-1} on a Thermo Electron Corporation model Nexus 670 spectrometer equipped with FT-Raman module accessory. The FT-IR spectrum of IPDP was recorded in the frequency region 4000-400 cm^{-1} on a Nexus 670 spectrometer equipped with an MCT detector, a KBr pellet technique.

2. COMPUTATIONAL DETAILS

The molecular geometry optimization and vibrational frequency calculations were carried out for,IPDP with GAUSSIAN 09W [1] package the density functional theory used in B3LYP i.e. Becke's three-parameter hybrid functional with the Lee-Yang-Parr correlation functional methods [2,3] with 6-31+G (d) and 6-311++G (d, p) basis sets. Scaling of the force field was performed according to the scaled quantum mechanical (SQM) procedure [4]. The calculated potential energy distribution (PED) and predicted IR and Raman intensities were done on a PC with the Version V7.0 of the MOLVIB program written by Sundius [5,6]. To achieve a close agreement between observed and calculated frequencies, the least-square fit refinement algorithm was used. By combining the results of the GUASSVIEW [7] program with symmetry considerations, along with the available related molecules, vibrational frequency assignments were made with a high degree of accuracy.

II. PREDICTION OF RAMAN INTENSITY

The Raman activities (S_R) calculated with the Gaussian 09W Program were converted to Raman intensities (I_R) using the following relationship derived from the intensity theory of Raman scattering [8-9].

$$I_R = \frac{f(\upsilon_0 - \upsilon_i)^4 S_R}{\upsilon_i[1 - \exp(-hc\upsilon_i / kT)]}$$

where υ_0 is the laser exciting frequency in cm^{-1} (in this work, we have used the excitation wavenumber υ_0=9392.4 cm^{-1}, which corresponds to the wavelength of 1064 nm of a Nd:YAG laser), υ_i is the vibrational wavenumber of the ith normal mode (in cm^{-1}) and S_R is the Raman scattering activity of the normal mode υ_i, f (is the constant equal to 10^{-12}) is a suitably chosen common normalization factor for all peak intensities. h, k, c, and T are Planck constant, Boltzmann constant, speed of light, and temperature in Kelvin, respectively.

III. POLARIZABILITY AND HYPERPOLARIZABILITY

The polarizability (α) and the first-order hyperpolarizability (β_0) of this novel molecular system and the electric dipole moment (μ) of the IPDP were calculated using B3LYP method with 6-31+G (d) and 6-311++G (d, p) basis sets, based on the finite field approach. In presence of an applied electric field, the energy of a system is a function of the electric field. Polarizability and hyperpolarizability characterize the response of a system in an applied electric field [10]. The first hyperpolarizability is a third-rank tensor that can be described by a 3×3×3 matrix. The 27 components of the 3D matrix can be reduced to 10 components due to the Kleinman symmetry [11]. The components of β_0 are defined as the coefficients in the Taylor series exponents the energy in the external electric field. When the external electric field is weak and homogeneous, this expansion becomes:

$$E = E^0 - \frac{\mu_i F_i}{1!} - \frac{\alpha_{ij} F_i F_j}{2!} - \frac{\beta_{ijk} F_i F_j F_k}{3!} - \frac{\gamma_{ijkl} F_i F_j F_k F_l}{4!} + \cdots$$

where E is the energy of the unperturbed molecules, F_i is the field at the orgin and μ_i, α_{ij}, β_{ijk} and γ_{ijkl} are the components of diple moment, polarizability and the hyperpolarizability, respectively. The total static dipole moment (μ), the mean polarizability (α_0), the anisotropy of the polarizability $\Delta\alpha$ and the mean first hyperpolarizability (β_0), using the x, y, z components they are defined as:

The total static dipole moment is

$$\mu = (\mu_x^2 + \mu_y^2 + \mu_z^2)^{\frac{1}{2}}$$

The isotropic polarizability is

$$\alpha = \frac{\alpha_{xx} + \alpha_{yy} + \alpha_{zz}}{3}$$

The polarizability anisotropy invariant is

$$\Delta\alpha = 2^{-1/2}[(\alpha_{xx} - \alpha_{yy})^2 + (\alpha_{yy} - \alpha_{zz})^2 + (\alpha_{zz} - \alpha_{xx})^2 + 6\alpha_{xx}^2]^{1/2}$$

The average hyperpolarizability

$$\beta_{tot} = (\beta_x^2 + \beta_y^2 + \beta_z^2)^{1/2}$$

Where

$$\beta_x = (\beta_{xxx} + \beta_{xyy} + \beta_{xzz})$$
$$\beta_y = (\beta_{yyy} + \beta_{xxy} + \beta_{yzz})$$
$$\beta_z = (\beta_{zzz} + \beta_{xxz} + \beta_{yyz})$$

since the values of the polarizability and the hyperpolarizability of the Gaussian 09W output are reported in atomic units (a.u.), the calculated values have been converted into electrostatic units (e.s.u.) (1 a.u.=0.3728 $\times 10^{-30}$ e.s.u.). The total molecular dipole moment (μ) are 3.6992 debye (D), 3.6992 debye and calculated mean polarizabilty values are 0.3728×10^{-30} and 0.83223×10^{-30} e.s.u. in B3LYP method with 6-31+G (d) and 6-311++G (d, p) values are presented in Table 1. The hyperpolarizability of IPDP ipomparing with both basis sets, the B3LYP/6-311++G (d, p) are greater than the B3LYP/6-31+G (d) method.

Table 1. The eectric dipoe moment(μ) (debye), the mean poarizabiity(α)(e.s.u.), anisotropy poarizabiity(Δα)(e.s.u.) and first hyperpoarizabiity(β_{tot})(e.s.u.) for 4,4-isopropylidenebis (2,6-dichlorophenol) at B3LYP/6-31+G (d) and B3LYP/6-311++G (d, p) methods.

Parameters	B3YLP/6-31+G (d)	B3LYP /6-311++G (d, p)
μ_x	2.7016	2.6415
μ_y	-2.0020	-2.0218
μ_z	-1.5421	-1.4775
μ	3.69928	3.6398
α_{xx}	-167.6715	-167.8261
α_{xy}	4.2591	4.2965
α_{xz}	3.2649	3.0043
α_{yy}	-146.0549	-145.7778
α_{yz}	-0.9535	-0.9365
α_{zz}	-131.5547	-131.5179
α	-148.4270	-148.3739
$\Delta\alpha$	225.2266	319.1155
β_{xxx}	54.1658	53.3417
β_{yyy}	0.9149	1.0048
β_{zzz}	-0.6871	-0.8797
β_{xyy}	4.4006	3.2101
β_{xxy}	-7.5141	-7.8797
β_{xxz}	-85.8502	-84.4016
B_{xzz}	-10.0407	-8.8401
β_{yzz}	0.2298	0.0152
β_{yyz}	-4.3713	-4.3362
β_{xyz}	1.6860	1.6533
β_{tot}	2.9795×10^{-30}	2.2323×10^{-30}

IV. RESULTS AND DISCUSSION

4.1. Molecular geometry

In order to obtain the stable optimization geometry, the self consistent field (SCF) energy calculation is performed on the fifteen possible structures of optimization steps as shown in Fig. 1. The possibility of optimization geometry is found by locating NCO group of the title molecule in different orientations. The position of NCO group in different orientations gives rise to fifteen possible optimizations. Most of the more complicated structures have free internal structural parameter, which can either be taken from experiment or optimized using the calculated forces on the nuclei. Most optimization algorithm estimated or computed the value of the second derivative Hessian matrix of the energy with respect to the molecular coordinates, updating the matrix of force constants. The force constants specify the curvature of the surface at the point, which provides additional information useful for determining the next step. The predicted geometrical parameters such as, bond lengths, bond angles and dihedral angles of IPDP calculated at B3LYP/6-31+G (d) and B3LYP/6-311++G (d, p) level of theory are presented in Table 2 in accordance with atom numbering schemes given in Fig. 2. Since the exact crystal structure of IPDP is not available till now, the optimized structure can only be compared with other similar system for which the crystal structure have been solved. For comparative purpose, the theoritical data [4] are also presented. From the theoretical values we can find that most of the optimized bond lengths and bond angles are slightly larger or shorter than experimental values. Optimized structure yields fairly accurate bond length pairs for the bonds C_1-C_6, C_2-C_3, C_6-H_{14} at DFT level of calculations. The values of bond lengths C_2-H_{10}, C_3-C_4, C_5-C_6, C_5-C_{13}, O_7-H_8, and H_8-Cl_9 are greater than literature values. The ring angle C_4-C_5-C_6 is slightly less than ring angle C_1-C_2-C_3. The breakdowns of hexagonal structure of the aromatic ring are obvious from the value of dihedral angles O_7-C_1-C_2-H_{10} and O_7-C_1-C_6-H_{14} are less than the literature values. Compared with B3LYP/6-31+G (d) and B3LYP/6-311++G (d, p) level of the bond lengths, bond angles and dihedral angles differences between theoretical approaches have been shown in Figs.3,4, (Supplementary Materials) respectively. Optimization geometry is use to find the local minimum structure (LMS), global minimum structure (GMS) and the transition state structure (TSS). The optimized energy, maximum force and root mean square (RMS) force are presented in Table 2

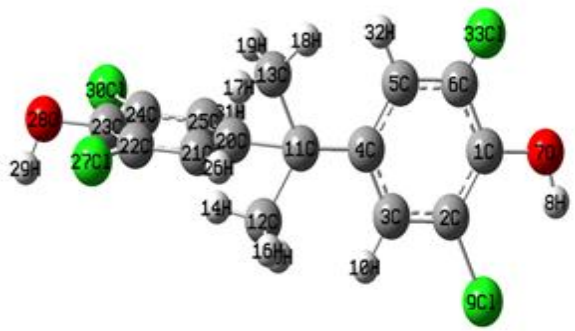

Fig.1. Possible conformational structures of of 4,4- isopropylidenebis(2,6-dichlorophenol)

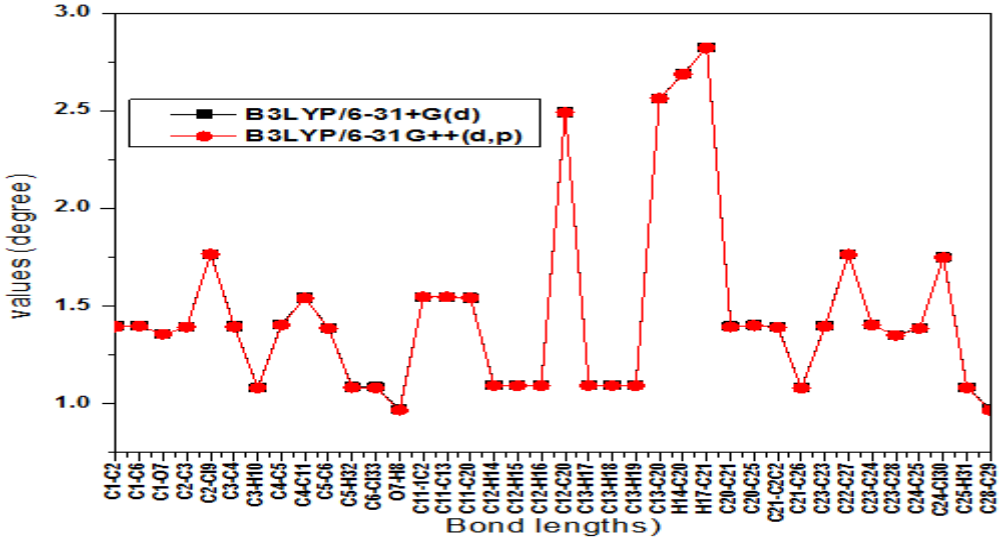

Fig.2. Bond length difference between the theoretical B3LYP/6 4,4- isopropylidenebis (2,6dichlorophenol)

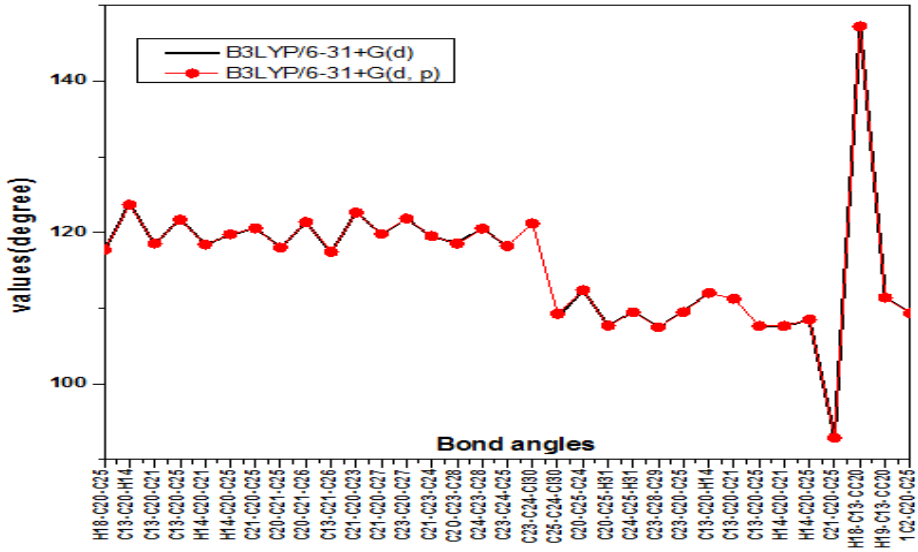

Fig.3. Bond angle differences between experimental and theoretical B3LYP/6-31+G (d) and B3LYP/6-311++G (d, p) of the 4,4-isopropylidenebis (2,6-dichlorophenol)

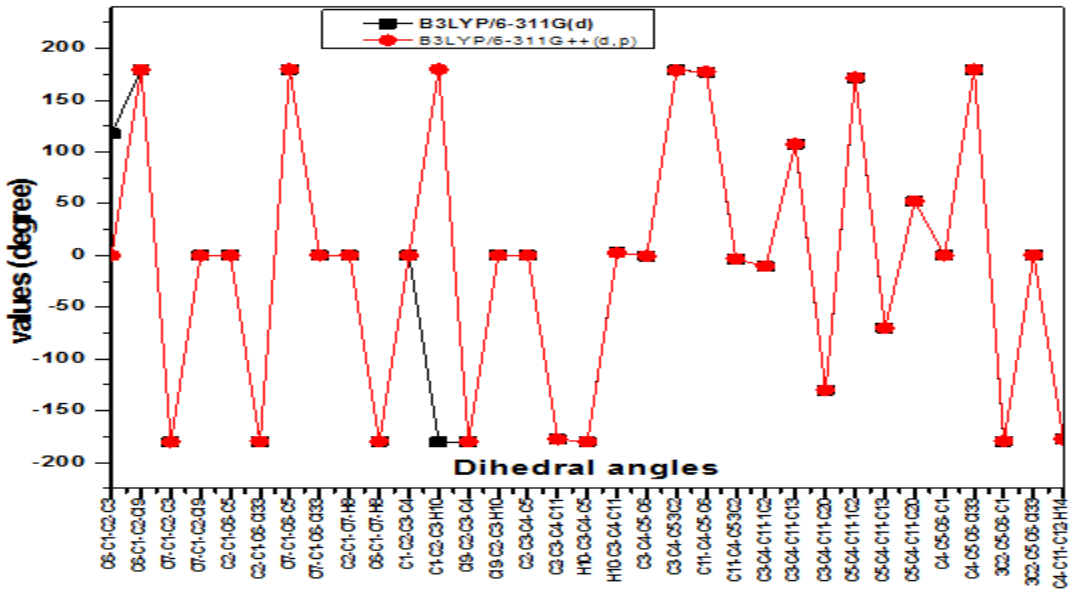

Fig.4. Dihedral angle differences between experimental and theoretical B3LYP/6-31+G (d) and B3LYP/6-311++G (d, p) of the 4 isopropylidenebis (2,6-dichlorophenol)

Table 2. Optimized geometrical parameters of 4,4-isopropylidenebis (2,6-dichlorophenol) by B3LYP/6-31+G (d) and B3LYP/6-311++G (d, p) methods.

Bond Lengths	Bond angles		Values (degrees)					
	B3LYP		Bond angles	B3LYP		Dihedral angles	B3LYP	
	6-31+G (d)	6-311++G (d, p)		6-31+G (d)	6-311++G (d, p)		6-31+G (d)	6-311++G (d, p)
C1-C2	1.399	1.395	H18-C20-C25	117.64	117.74	C6-C1-C2-C3	117.65	-0.203
C1-C6	1.401	1.398	C13-C20-H14	123.92	123.68	C6-C1-C2-Cl9	179.75	179.658
C1-O7	1.356	1.357	C13-C20-C21	118.44	118.56	O7-C1-C2-C3	-179.98	-179.959
C2-C3	1.395	1.393	C13-C20-C25	121.83	121.71	O7-C1-C2-Cl9	-0.06	-0.098
C2-Cl9	1.768	1.766	H14-C20-C21	118.44	118.43	C2-C1-C6-C5	0.10	0.135
C3-C4	1.397	1.395	H14-C20-C25	119.74	119.774	C2-C1-C6-Cl33	-179.58	-179.548
C3-H10	1.083	1.081	C21-C20-C25	120.60	120.587	O7-C1-C6-C5	179.92	179.904
C4-C5	1.407	1.404	C20-C21-C25	118.05	118.023	O7-C1-C6-Cl33	0.C24	0.221
C4-C11	1.542	1.541	C20-C21-C26	121.35	121.390	C2-C1-O7-H8	0.18	0.195
C5-C6	1.388	1.386	C13-C21-C26	117.45	117.468	C6-C1-O7-H8	-179.64	-179.559
C5-H32	1.086	1.084	C21-C20-C23	122.72	122.668	C1-C2-C3-C4	0.03	0.046
C6-Cl33	1.086	1.083	C21-C20-C27	119.78	119.825	C1-C2-C3-H10	-179.98	179.994
O7-H8	0.973	0.967	C23-C20-C27	121.90	121.871	Cl9-C2-C3-C4	-179.89	-179.814
C11-1C2	1.548	1.547	C21-C23-C24	119.41	119.551	Cl9-C2-C3-H10	0.10	0.134
C11-C13	1.548	1.547	C2O-C23-C28	118.68	118.574	C2-C3-C4-C5	0.17	0.176
C11-C20	1.542	1.542	C24-C23-C28	120.58	120.532	C2-C3-C4-C11	-177.35	-177.534
C12-H14	1.095	1.092	C23-C24-C25	118.13	118.238	H10-C3-C4-C5	-179.82	-179.770
C12-H15	1.095	1.092	C23-C24-Cl30	121.C30	121.230	H10-C3-C4-C11	2.67	2.520
C12-H16	1.096	1.093	C25-C24-Cl30	108.77	109.284	C3-C4-C5-C6	-0.C24	-0.245
C12-C20	2.493	2.492	C20-C25-C24	112.39	112.407	C3-C4-C5-C2	179.02	178.979
C13-H17	1.096	1.094	C20-C25-H31	107.69	107.711	C11-C4-C5-C6	177.35	177.533
C13-H18	1.095	1.092	C24-C25-H31	109.57	109.476	C11-C4-C5-C2	-3.39	-3.243
C13-H19	1.095	1.092	C23-C28-C29	107.50	107.499	C3-C4-C11-C2	-10.62	-10.292
C13-C20	2.564	2.564	C23-C20-C25	109.61	109.511	C3-C4-C11-C13	107.58	107.945
H14-C20	2.690	2.688	C13-C20-H14	112.03	112.049	C3-C4-C11-C20	-130.17	-129.808
H17-C21	2.824	2.823	C13-C20-C21	111.o28	111.262	C5-C4-C11-1C2	171.92	172.051
C20-C21	1.397	1.394	C13-C20-C25	107.68	107.665	C5-C4-C11-C13	-69.88	-69.713
C20-C25	1.404	1.401	H14-C20-C21	107.66	107.682	C5-C4-C11-C20	52.37	52.534

C21-C22	1.394	1.391	H14-C20-C25	108.42	108.511	C4-C5-C6-C1	0.11	0.090
C21-C26	1.083	1.081	C21-C20-C25	92.96	92.887	C4-C5-C6-Cl33	179.78	179.763
C23-C23	1.400	1.396	H18-C13-CC20	147.C27	147.246	3C2-C5-C6-C1	-179.16	-179.141
C22-C27	1.766	1.765	H19-C13-CC20	111.48	111.435	3C2-C5-C6-Cl33	0.51	0.532
C23-C24	1.406	1.403	1C2-C20-C25	109.39	109.321	C4-C11-C12-H14	-177.53	-177.555
C23-C28	1.351	1.351	C13-C20-H14	112.07	112.083	C4-C11-C12-H15	-58.06	-58.158
C24-C25	1.388	1.386	C13-C20-C21	107.65	107.668	C4-C11-C12-H16	63.50	63.521
C24-Cl30	1.750	1.749	C13-C20-C25	108.48	108.565	C13-C11-C12-H14	64.15	64.084
C25-H31	1.085	1.083	H14-C20-C21	94.04	93.994	C13-C11-C12-H15	-176.38	-176.519
C28-C29	0.973	0.967	H14-C20-C25	107.61	107.599	C13-C11-C12-H16	-54.82	-54.841
			C21-C20-C25	143.20	143.127	C4-C11-C13-H17	-176.18	-176.271
			C20-C21-C22	92.47	92.541	C4-C11-C13-H18	-57.C24	-57.378
			C20-C21-C26	53.94	53.871	C4-C11-C13-H19	62.01	61.832
			C2C2-C21-C26	122.88	122.845	1C2-C11-C13-H17	-54.87	-54.921
			C21-C2C2-C23	119.34	119.336	1C2-C11-C13-H18	64.07	63.972
			C21-C2C2-C27	59.13	59.114	1C2-C11-C13-H19	-176.68	-176.819
			C23-C2C2-C27	125.92	126.118	C4-C11-C20-H14	145.84	145.858
			C2C2-C23-C24	102.62	102.522	C4-C11-C20-C21	-130.09	-129.737

4.2.Vibrational spectral analysis

The optimized structural parameters were used to compute the vibrational frequencies of IPDP at the DFT (B3LYP)/6-31+G (d) and 6-311++G (d, p) level of calculation. The title molecule contains 33 atoms and belongs to C_1 symmetry point group. Hence the number of normal modes of vibrations for IPDP works to 93. Of the normal modes of vibrations, 63 modes of vibrations are in-plane modes and 30 modes of vibrations are out-of-plane modes are represented.

All the 93 fundamental vibrations are active in Raman scattering and infrared absorption. Detailed description of vibrational modes can be given by means of normal coordinate analysis. Comparison of the frequencies calculated at B3LYP/6-31+G (d) and B3LYP/6-311++G (d, p) levels with experimental values reveals the over estimation of the calculated vibrational modes. Inclusion of certain extent makes the B3LYP/6-311++G (d, p) values smaller in comparison to the B3LYP/6-31+G (d) frequency data. Reduction in computed harmonic vibrational frequencies through basis set sensitive are only marginal as observed in the DFT values using 6-311++G (d, p). Anyway, notwithstanding the level of calculations, it is customary to scaling down the computed harmonic frequencies in order to good improve the agreement with the experimental data.
Root mean square (RMS) values of frequencies were obtained in the study using the following experessions.

$$RMS = \sqrt{\frac{1}{n-1}\sum_{i}^{n}(\upsilon_i^{calc} - \upsilon_i^{exp})^2}$$

The RMS error between unscaled and experimental frequencies is 103 cm^{-1} by B3LYP/6-31+G (d) and 81 cm^{-1} by B3LYP/6-311++G (d, p). However, for reliable information on the vibrational properties the use of a selective scaling is necessary. The calculated frequencies are scaled using the set of transferable scale factors recommended by Rauhut and Pulay [12] and resulted in a RMS deviation of 7 cm^{-1} by B3LYP/6-31+G (d) and 5 cm^{-1} by B3LYP/6-311++G (d, p). The observed FT-IR and FT-Raman spectra of the title molecule along with the simulated IR and Raman spectra are shown in Figs. 5 respectively. The observed FT-IR, FT-Raman wavenumbers and the calculated wavenumbers using density functional B3LYP method with 6-31+G (d) and 6-311++G (d, p) basis sets along with their relative intensities, probable assignments of the compound are summarized in Table 3.

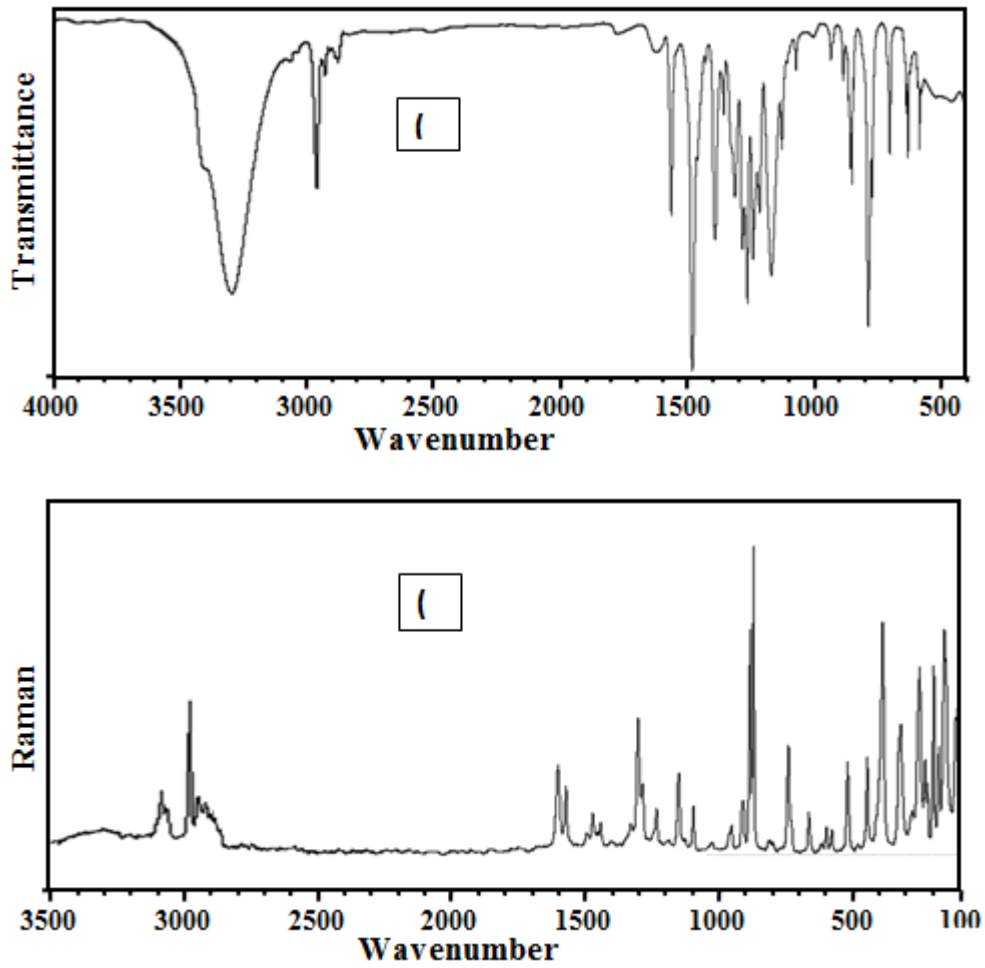

Fig. 5. Observed (a) FT-IR and (b) FT-Raman spectra of 4, 4-isopropylidenebis (2,6-dichlorophenol)

Table 3. Vibrational assignments of FT-IR and FT-Raman peaks along the theoreticallay computed wavenumbers, IR intensity (I_{IR}) and Raman intensity (I_{Raman}) and the percentage of potential energy distribution.

S.No	Species	Observed wave number (cm^{-1})		Cacuated wave number (cm^{-1})								Assignments with % of PED[c]
		FT-IR	FT-Raman	B3YP/6-31+G (d)				B3LYP/6-311`++G (d, p)				
				Unscaed	Scaed[b]	I_{IR}	I_{Raman}	Unscaed	Scaed[b]	I_{IR}	I_{Raman}	
1	A			3699	3507	76.17	94.374	3768	3505	83.87	101.93	υO-H(97)
2	A			3697	4498	101.08	80.033	3763	3499	75.10	122.04	υO-H(99)
3	A		3073	3244	3080	00.30	48.875	3219	3071	46.85	0.09	CH3 ass(98)
4	A		3068	3238	3070	0.67	50.776	3214	3065	49.99	0.19	CH3 ass(99)
5	A			3221	3065	0.80	42.379	3196	3062	43.47	0.29	CH3ass(98)
6	A			3220	3060	5.16	127.941	3195	3059	136.88	2.91	CH3 ass(97)
7	A			3198	3040	8.31	40.455	3175	3036	39.28	6.34	υCH(97
8	A			3132	3028	28.13	70.810	3106	3027	66.23	26.75	υCH(99)
9	A	2968		3132	3026	5.16	67.801	3105	3025	54.09	21.08	υCH(98)
10	A	2958	2958	3124	2963	8.31	101.420	3099	2960	113.98	52.21	υCH(97)
11	A	2848		3119	2957	6.93	25.276	3094	2950	22.84	4.90	υCH(97)
12	A	2943		3056	2942	18.90	215.679	3033	2942	307.25	19.97	CH3ass(97)
13	A	2924	2918	3051		19.22	13.022	3028		17.60	19.00	CH3(98)
15	A			1651	1600	1.72	50.778	1633	1598	47.63	1.17	υCC(87)
16	A	1580		1629	1579	24.33	5.959	1612	1576	7.53	19.43	υCC(86)

17	A		1561	1615	1570	42.33	9.080	1599	1568	10.70	45.23	υCC (83)
18	A	1498		1549	1497	153.46	4.775	1528	1496	4.12	166.39	υCC (78)
19	A		1491	1540	1493	8.40	24.119	1514	1491	1.79	91.82	CH3 ibp (86)
20	A			1539	1488	26.96	7.996	1511	1486	11.80	14.93	CH3 ibp (87)
21	A			1532	1481	124.21	1.403	1508	1476	1.32	108.94	υCC (80)
22	A		1451	1524	1453	51.74	0.937	1497	1449	0.45	20.40	υCC (80)
23	A		1446	1516	1449	5.26	20.234	1489	1442	7.58	3.68	υCC (78)
24	A			1457	1419	6.64	0.956	1437	1412	1.60	6.56	υCC (80)
25	A			1449	1407	13.39	2.886	1427	1409	0.43	36.85	υCC (99)
26	A	1403		1442	1400	29.83	1.579	1421	1403	0.98	8.58	CH3opb (77)
27	A	1378		1424	1381	17.30	3.636	1399	1376	0.38	16.55	CH3 opb (73)
28	A		1328	1387	1333	38.47	5.690	1364	1327	6.943	27.52	υCC (73)
29	A	1313		1379	1317	81.76	4.181	1356	1310	5.51	62.50	βCH (65)
30	A	1296	1296	1343	1303	95.97	12.258	1320	1301	16.95	100.64	βCH (67)
31	A		1292	1333	1296	48.84	14.553	1311	1290	22.47	64.06	CH3 sy (63)
32	A	1268		1302	1271	43.71	2.669	1281	1272	8.32	44.19	CH3 sy (76)
33	A	1240		1292	1243	52.29	1.446	1270	1240	2.37	42.85	υC-O (78)
34	A	1223	1222	1266	1227	31.28	3.160	1251	1220	1.65	31.32	υC-O (79)
35	A			1253	1210	26.07	5.691	1239	1207	6.40	20.52	β CH (53)
36	A			1228	1192	191.25	2.193	1209	1193	3.41	180.55	β CH (54)
37	A	1162		1207	1183	138.52	1.707	1190	1180	2.11	137.81	β OH (62)
38	A			1181	1167	1.65	2.878	1169	1163	3.09	1.29	υCC (67)
39	A		1136	1163	1139	13.13	9.886	1149	1135	12.93	15.93	β OH (61)
40	A			1153	1129	3.88	7.173	1141	1127	7.33	3.17	CH3 ipr (56)
41	A			1129	1110	0.40	5. 904	1117	1107	8.64	0.93	CH3 ipr (55)
42	A		1089	1102	1091	1.56	4.374	1093	1087	5.53	0.65	υCC (68)
43	A		1009	1065	1012	21.60	1.445	1060	1013	1.51	20.98	υCC (67)
44	A	998			999	0.87	2.533	1028	998	0.63	0.56	υCC(68)
45	A	960		966	954	0.96	2.087	971	957	0.22	0.19	β CCC (55)
46	A		945	955	946	1.46	5.088	946	947	5.64	7.44	β CCC (54)
47	A			954	943	7.34	7.095	945	942	4.44	1.50	β C-O (52)
48	A	906	903	911	907	5.74	0.804	907	904	0.33	4.95	β C-O (53)
49	A			900	892	9.67	5.889	894	890	4.70	7.21	CH3 opr(50)
50	A	877		892	870	8.40	2.443	887	869	1.90	10.50	CH3 opr (47)
51	A	871	865	883	863	16.42	3.369	879	865	2.98	18.24	γ CH (46)
52	A			870	862	3.41	31.591	865	860	39.82	3.83	γ CH (47)
53	A	803		844	804	17.06	2.842	837	800	0.71	20.18	γ CH (47)
54	A	782		796	782	80.72	2.109	792	780	1.37	103.03	γ CH (47)
55	A			794	783	43.30	1.019	789	780	1.44	27.66	υC-Cl (78)
56	A			729	710	10.43	15.423	726	708	17.87	12.14	υC-Cl (78)
57	A		712	726	706	6.54	2.624	722	703	3.46	7.73	υC-Cl (78)
58	A		706	718	702	9.00	0.542	712	700	0.64	12.65	υC-Cl (77)
59	A			683	676	14.19	7.051	681	672	6.12	13.96	γ O-H (48)
60	A	643	648	656	650	3.62	3.354	650	649	2.72	4.02	γ O-H (47)
61	A	617	612	625	620	8.67	2.449	616	610	2.57	11.65	β CCC (53)
62	A	590	591	593	594	22.67	0.542	590	590	0.68	24.68	β CCC (53)
63	A	562	560	566	556	8.16	5.378	564	518	3.94	6.19	β CCC (52)
64	A			527	520	7.67	2.104	525	502	1.40	7.66	β CCC (51)
65	A		503	508	503	0.50	1.145	503	490	1.34	1.93	β CCC (50)
66	A			501	493	2.77	12.175	498	468	11.53	1.45	γ CCC (48)
67	A		471	480	469	9.48	1.632	479	436	2.16	9.52	γ CCC (47)
68	A		440	449	437	0.52	0.174	448	414	0.12	0.45	CH3 twist (46)
69	A			429	413	4.18	3.899	429	408	2.83	1.95	β C-Cl (43)
70	A			419	409	102.42	2.747	409	396	1.81	83.23	β C-Cl (47)
71	A		397	417	400	111.27	2.601	401	381	1.43	99.15	CH3 twist

												(37)
72	A			389	380	1.75	1.829	386	378	2.32	3.15	β C-Cl (40)
73	A			384	379	1.19	2.699	382	368	1.49	4.05	β C-Cl (42)
74	A			378	370	1.60	5.950	377	368	5.40	1.47	γ CCC (43)
75	A			340	333	1.33	0.975	335	332	1.18	2.06	γ CCC (43)
76	A			330	327	0.48	1.415	325	326	2.02	0.46	γ CCC (44)
77	A		308	322	308	1.22	2.400	317	206	2.79	1.30	γ CCC (42)
78	A			302	297	4.71	0.444	295	296	0.48	4.55	γ CC (40)
79	A			293	286	0.71	1.202	287	287	1.35	0.84	γ C-O (44)
80	A		273	286	278	3.07	1.117	280	277	1.45	3.33	γ C-Cl (41)
81	A		250	264	753	0.44	1.125	262	752	1.47	0.51	γ C-Cl (43)
82	A		223	251	219	0.46	0.512	248	218	0.47	0.63	γ C-Cl (48)
83	A			219	210	0.43	1.341	214	207	0.95	0.21	γ C-Cl ()
84	A		200	207	201	0.27	2.444	205	196	2.04	0.20	γ C-Cl ()
85	A		176	179	173	0.05	2.736	176	169	1.95	0.03	γ C-O ()
86	A			170	167	0.10	0.661	167	163	0.55	0.22	γ CCC (43)
87	A		150	158	148	0.09	1.615	156	143	1.44	0.12	γ CCC (44)
88	A			138	133	0.01	2.079	136	105	1.72	0.02	γ CCC (42)
89	A			109	108	0.06	0.214	106	107	0.16	0.08	γ CC (40)
90	A			101	97	0.19	0.496	99	96	0.33	0.11	γ CCC (43)
91	A			43	42	0.05	6.439	42	41	4.92	0.03	γ CCC (44)
92	A			23	20	0.02	4.047	21	20	3.18	0.01	γ CCC (42)
93	A			21	19	0.03	2.637	18	18	1.91	0.05	γ CC (40)

4.3. Vibrational assignments:

Aromatic ring breathing modes

Benzene ring is frequently encountered in organic chemistry. Although we write benzene as a six-membered ring with three double bonds, this is not a good representation of the structure of the molecule. The vibrational motions of a benzene ring are not isolated but involve the entire molecule. To describe one of the fundamental motions of benzene, consider some imaginary lines passing through the centre of the molecule and extending out through each carbon atom and beyond. A symmetric stretching and compression of all the carbon atoms of benzene along each line is an example of the ring breathing motion. Simultaneous expansions and compressions of these six carbon atoms lead to other ring-breathing motions [13]. The ring C=C and C-C stretching vibrations, known as semicircle stretching modes usually occurs in the region 1580cm^{-1} [14-15]. In general, the bands are of variable intensity and are observed 1590-1575 cm^{-1}, 1540-1470 cm^{-1}, 1465-1430 cm^{-1} and 1380-1280 cm^{-1} from the frequency ranges given by Varsanyi [16] for the five bands in the region. In the present work, the frequencies observed in FT-IR spectrum at 1585, 1552, 1521, 1424 and 1296 cm^{-1} have been assigned to C-C stretching vibrations. The corresponding vibration appears in the FT-Raman spectrum at 1606, 1561, 1451,1446, 1398 and 1296cm^{-1}. All the bands lie in the expected range when compared to the literature values. The C-C aromatic stretch, known as semicircle stretching, predicted at 1556 cm^{-1} is in reasonable agreement with the band observed at 1552 and 1550 cm^{-1} in FT-IR and FT-Raman spectra. The CCC in-plane bending vibrations observed at 998, 960, 567 and 541 cm^{-1} in FT-IR spectra. The corresponding values appear in the FT-Raman spectra at 909, 878, 564 and 536 cm^{-1}. The CCC out-of-plane bending vibrations appeared at 308 cm^{-1}. These assignments are in good agreement with the literature [17,18]. These observed frequencies show that, the substitutions in the benzene ring to some extend affect the ring modes of vibrations. The theoretically computed values by B3LYP/6-31+G (d) and B3LYP/6-311++G (d, p) methods are in good agreement with experimental values.

C-H vibrations

Consider the carbon-hydrogen stretching frequencies. If we assume that all C-H stretching force constants are similar in magnitude, we would expect the stretching frequencies of all C-H bonds to be similar. This expectation is based on the fact that the mass of a carbon atom and whatever else is attached to the carbon is much larger than the mass of hydrogen. The reduced mass for vibration of a hydrogen atom would be approximately the mass of hydrogen atom that is independent of the structure. All C-H stretching modes are observed at approximately 3000 cm^{-1}, exactly as expected. Fortunately, the force constants do vary with structure in a fairly predictable manner, and therefore it is possible to differentiate between different types of C-H bonds. Generally, the aromatic C-H vibrations are normally found between 3100-3000 cm^{-1} [19, 20]. However, as with any complex molecule, vibration interactions occur and these levels only indicate the predominant vibration. Substituted benzenes, i.e., bonds whose position is significantly affected by the mass and electronic properties, mesmeric or inductive of the substituent. Since, IPDP is a tri-substituted aromatic system; it has three C-H moiety. The aromatic structure shows the

presence of C-H stretching vibrations assigned at 3073, 3068 cm^{-1} in FT-IR spectra and 3040, and 3028cm^{-1} in FT-Raman spectra. The aromatic C-H in-plane bending modes of benzene and its derivatives are observed in the region 1300-1000 cm^{-1} [21]. These modes are in the FT-IR spectrum of the title molecule at 1313, 1223, and 1023 cm^{-1} and the corresponding modes are identified in the FT-Raman spectrum at 865 ,860 and 806 cm^{-1}. The out-of-plane bending mode of benzene derivatives are generally observed in the region 1000-600 cm^{-1} [22]. Accordingly to the PED results, the prominent absorption peaks at 998, 960, 877,and 712 cm^{-1} in FT-IR and 877, 870,860 and 804 cm^{-1} in FT-Raman are assigned to C-H out-of-plane bending modes were also assigned within the characteristic region and are presented in Table 6, respectively.

C-Cl vibrations

The C-C*l* stretching vibrations give generally strong bands in the region 800-600 cm^{-1} [23]. The vibrations belonging to the bond between the ring and halogen atoms were worth the discussion here since the mixing of vibrations are possible due to the lowering of the molecular symmetry and the presence of heavy atoms on the periphery of molecule [24]. In the present study, C-C*l* stretching vibration observed at 782 and 784 cm^{-1} in FT-IR spectra and corresponding modes are identified in the FT-Raman spectrum at 808, 776 and 674 cm^{-1}. The C-C*l* in-plane bending mode of DCPI is observed at 442 cm^{-1} in FT-IR and 438 and 318 cm^{-1} in FT-Raman spectrum. The band observed at 250, 223 and 200 cm^{-1} in FT-Raman is due to C-C*l* out-of-plane bending. These assignments are in good agreement with the literature [25,26] as well as computed values by B3LYP method with 6-31+G (d) and 6-311++G (d, p) basis sets.

Methyl vibrations

Methyl groups are generally referred to an electron-donating substituent's in the aromatic ring system. For the assignments of CH_3 group frequencies on can expect nine fundamentals can be associated to each CH_3 group, namely the asymmetrical stretching (CH_3ass), symmetrical stretching (CH_3ss), in-plane bending (CH_3ipb), out-of-plane bending (CH_3opb), symmetric bending (CH_3sb), in-plane rocking (CH_3ipr), out-of-plane rocking (CH_3opr) and twisting (CH_3twist) modes. Whenever a methyl group is present in a compound, it gives rise to two asymmetric and one symmetric stretching is usually at higher wavenumber than the symmetric stretching. The asymmetric stretching vibrations of CH_3 are expected in the region 3000−2925 cm^{-1} and symmetric CH_3 stretching vibrations in the range 2940−2905 cm^{-1} [27,28]. The observed asymmetric and symmetric stretching vibrations for CH_3 are at 3000 and 2966 cm^{-1} in FT-IR band and at 3000 and 2928 cm^{-1} in FT-Raman band. The calculated asymmetric and symmetric modes are 3073, 3068, 2958, and 2948 cm^{-1} at B3LYP 30803070, 3060 and 1296,1292 cm^{-1} at methods are good agreement with observed data's. Two bending modes can occur within a methyl group. The first of these, the symmetric bending vibration, involves the in-phase of C−H bonds. The second the asymmetric bending vibrations, involves out-of-phase of the C−H bonds. The CH_3 in-plane bending vibrations are expected in the region 1485−1400 cm^{-1} [29]. The FT-IR band observed at 1486 cm^{-1} and the out-of-plane bending vibration coupled with CH_3 in-plane bending vibration occurred at 1410 cm^{-1} in FT-IR spectrum. with the experimental values. The CH_3 symmetric bending mode observed at 1379 cm^{-1} in FT-IR value are good agreement with theoretical values (1396 and 1393 cm^{-1} the interaction with skeletal stretching modes. Generally, the in-plane and out-of-plane rocking modes observed in the region 1120−1050 cm^{-1} and 900−800 cm^{-1} [30,31]. In the present molecule, the FT-Raman spectra shows the band at 1112 cm^{-1} assigned to in-plane rocking and 826 cm^{-1} in FT-IR spectra are assigned to CH_3 out-of-plane rocking mode. As CH_3 twisting mode is expected below 400 cm^{-1}, the theoretically computed values are at 236, 182, 234 and 180 cm^{-1} in B3LYP and methods are assigned to mode, for, no spectral measurements were possible in the region due to instrumental limits. The C−CH_3 stretching vibration observed at 1006 cm^{-1} FT-Raman spectra and C−CH_3 in-plane and out-of-plane bending vibrations are observed at 573 and 257 cm^{-1} in FT-IR and FT-Raman spectrum, respectively.

4.4. Mulliken population analysis

The natural population analysis of DCPI obtained by Mulliken [33] population analysis with B3LYP level using different basis sets. Mulliken population analysis graph of DCPI are shown in Fig. 6. Mulliken atomic charge calculation has an important role in the application of quantum chemical calculation to molecular system because of atomic charge effect, dipole moment, molecular polarizability, electronic structure and a lot of properties of molecular systems. Mulliken atomic charges calculated at the B3LYP method with 6-31+G (d) and 6-311++G (d, p) basis sets are collected in Table4. It is worthy to mention that C_2, C_5, C_8, Cl_{10}, H_{11}, H_{12}, Cl_{13} and H_{14} atoms of DCPI exhibit positive charge, while C_1, C_3, C_4, C_6, N_7 and O_9 atoms exhibit negative charges. The maximum negative charge values of about -0.90251 in C_1 atom and C_2 has a maximum positive charge values of about 0.86181 in the molecule at B3LYP/6-31+G (d) and B3LYP/6-311++G (d, p) level of theory.

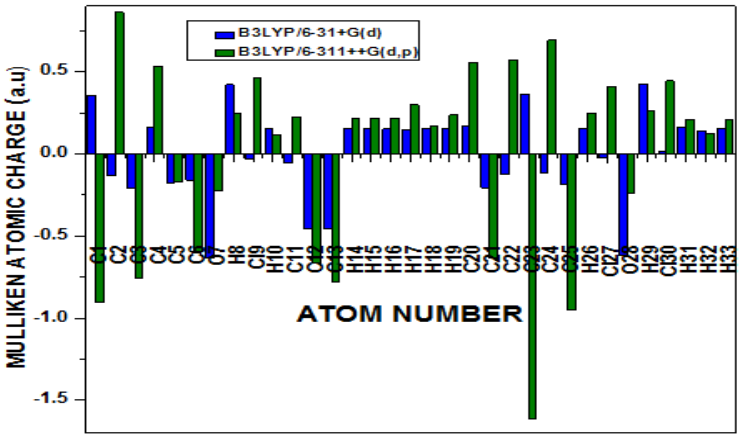

Fig. 6. Comparative Mulliken's plot by B3LYP/6-31+G (d) and B3LYP/6-311++G (d, p) Level 4, 4-isopropylidenebis (2,6 dichlorophenol)

Tabe 4. Mulliken's popuation anaysis of 4,4-isopropylidenebis (2,6-dichlorophenol) at B3lYP/6-31+G (d) and B3LYP/6-311++G (d, p)

S. No.	Atom No.	Mulliken's Atomic charges	
		B3YP/6-31+G (d, p)	B3LYP/6-311++G (d, p)
1	C_1	0.3551	-0.8017
2	C_2	-0.1307	0.9066
3	C_3	-0.2083	-0.6234
4	C_4	0.1614	0.3272
5	C_5	-0.1805	-0.5417
6	C_6	-0.1579	-0.3223
7	O_7	-0.6364	-0.1859
8	H_8	0.4219	0.2539
9	Cl_9	-0.0327	0.4533
10	H_{10}	0.1524	0.1732
11	C_{11}	-0.0553	0.0237
12	C_{12}	-0.4585	-0.5502
13	C_{13}	-0.4585	-0.5222
14	H_{14}	0.1561	0.1711
15	H_{15}	0.1563	0.1577
16	H_{16}	0.1505	0.1509
17	H_{17}	0.1485	0.1515
18	H_{18}	0.1578	0.1766
19	C_{19}	0.1543	0.1544
20	C_{20}	0.1680	-0.1518
21	C_{21}	-0.2071	-0.5278
22	C_{22}	-0.1242	0.9938
23	C_{23}	0.3626	-1.5504
24	C_{24}	-0.1163	0.8429
25	C_{25}	-0.1860	-0.9605
26	H_{26}	0.1557	0.1772
27	Cl_{27}	-0.0235	0.4507
28	O_{28}	-0.6178	-0.1180
29	H_{29}	0.4259	0.2496
30	Cl_{30}	0.0124	0.4721
31	H_{31}	0.1624	0.1913
32	H_{32}	0.1406	0.1706
33	Cl_{33}	0.1520	0.2077

methods.

4.5. Molecular electrostatic potentials (MEP)

Molecular electrostatic used extensively for interpreting potentials have been and predicting the reactive behavior of a wide variety of chemical system in both electrophilic and nucleophilic reactions, the study of biological recognition processes and hydrogen bonding interactions [32]. V(r), at a given point r(x,y,z) in the vicinity of a compound, is defined in terms of the interaction energy between the electrical charge generated from the compound electrons and nuclei and positive test charge (a proton) located at r. Unlike, many of the other quantities used at present, and earlier as indices of reactivity V(r) is a real physical property that can be determined experimentally by diffraction or by computational methods. For the systems studied the molecular electrostatic potential values were calculated as described previously, using the equation [33].

$$V(r) = \sum \frac{Z_A}{|R_A - r|} - \int \frac{\rho(r')}{|r' - r|} dr$$

where the summation runs over all the nuclei *A* in the compound and polarization and reorganization effects are neglected. Z_A is the charge of the nucleus *A*, located at R_A and $\rho(r')$ is the electron density function of the molecule.

To predict reactive sites for electrophilic and nucleophilic attack for the investigated compound, molecular electrostatic potential (MEP) was calculated at B3LYP/6-311++G (d, p) optimized geometries. The different values of the electrostatic potential at the surface are represented by different colors; red represents regions of most electro negative electrostatic potential, blue represents regions of the most positive electrostatic potential and green represents region of zero potential. Potential decreases in the order red < orange < yellow < green < blue. The MEP surface provides necessary information about the reactive sites. The electron total density onto which the electrostatic potential surface has been mapped is shown in Fig.7. The negative regions V(r) were related to electrophilic reactivity and the positive ones to nucleophilic reactivity. As easily can be seen in Fig.7, this figure provides a visual representation of the chemically active sites and comparative reactivity of atoms [34].

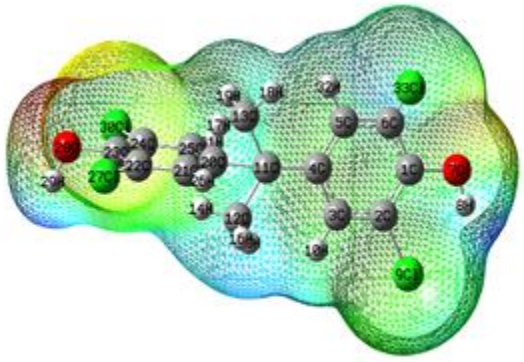

Fig. 7. Calculated 3D molecular electrostatic potential contour map of 4,4- isopropylidenebis (2,6-dichlorophenol)

4.6. Frontier molecular orbital's (FMOs)

The most important orbital's in molecule is the frontier molecular orbital's, called highest occupied molecular orbital (HOMO) and lowest unoccupied molecular orbital (LUMO). These orbitals determine the way of molecule interacts with other species. The frontier molecular energy gap helps to characterize the chemical reactivity and kinetic stability of the molecule. A molecule with a small frontier orbital gap is more polarizable and is generally associated with a high chemical reactivity, low kinetic stability and is also termed as soft molecule [35]. The low values of frontier orbital gap in IPDP it more chemical reactive and less kinetic stable. The frontier molecular orbital's plays an important role in the electric and optical properties [36]. The conjugated molecules are characterized by a small highest occupied molecular orbital – lowest unoccupied molecular orbital (HOMO – LUMO) separation, which is the result of a significant degree of intramolecular charge transfer from the end-capping electron acceptor groups through π – conjugated path [37]. The 3D plot of the frontier orbital's HOMO and LUMO of DCPI molecule is shown in Fig. 8. The positive phase is red and negative phase one is green (For interpretation of the reference to color in the text, the reader is referred to the web version of the article). Many organic molecules, conjugated π electrons are characterized by large values of molecular first hyperpolarizabilities, were analyzed by means of vibrational spectroscopy [38,39]. In most cases, even in the absence of inversion symmetry, the strongest band in the FT-Raman spectrum is weak in the FT-IR spectrum vice versa. But the intramolecular charge transfer from the donor-acceptor group in a single – double bond conjugated path can induce large variations of both the dipole moment and the polarizability, making FT-IR and FT-Raman activity strong at the same time. The analysis of wave function indicates that the electron absorption corresponds to the transition from the ground state to the excited state and is mainly described by one. An electron excitatio from the high

occupied molecular orbital to the lowest unoccupied molecular orbital (HOMO – LUMO) Generally, the energy gap between the HOMO and LUMO decreases, it is easier for the electrons of the HOMO to be excited. The higher energy of HOMO, the easier it is for HOMO to donate electrons whereas it is easier for LUMO to accept electrons when the energy of LUMO is low. The energy values of HOMO and LUMO levels are computed to be -0.20937 a.u. and -0.06573 a.u., respectively, and energy difference is -12,1888 a.u. in B3LYP/6-31+G (d). The energy values of HOMO and LUMO levels in B3LYP/6-311++G (d, p) is to be -0.20796 a.u. and -0.06420 a.u. and energy difference is 3.9119 a.u., respectively

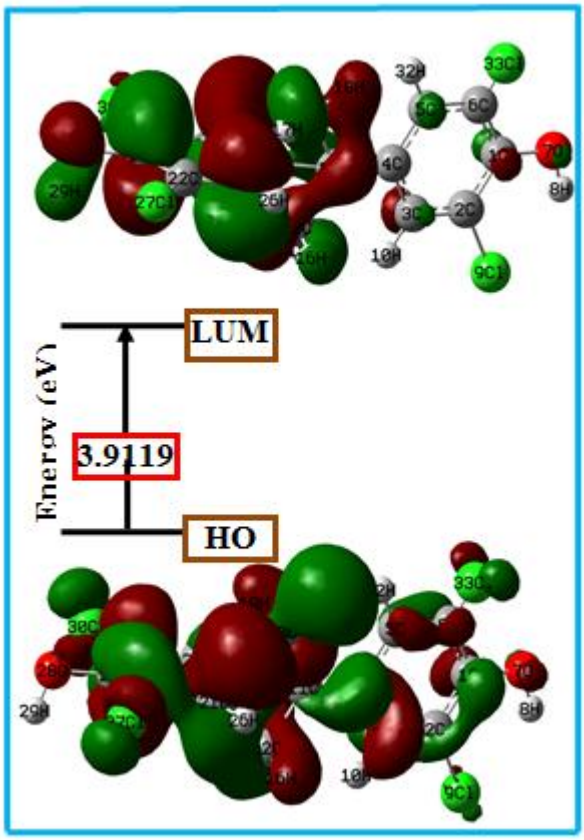

Fig. 8. The molecular orbitals and energies for the HOMO and LUMO of 4,4-isopropylidenebis (2,6-dichlorophenol)

Table 5. Comparison of HOMO, UMO energy gaps and reated moecuar properties of of 4,4-isopropylidenebis (2,6-dichlorophenol) at B3LYP/6-31+G (d) and B3LYP/6-311++G (d, p) methods.

Moecular properties	Energy (a.u.)	Energy gap (eV)	Ionization potentia (I)	Electron affinity (A)	Gobal Hardness (η)	Electro negativity (χ)	Globa softness (υ)	Chemical potentia (μ)	Gobal Electrophilicity (ω)
B3LYP/6-31+G(d)									
HOMO	-0.20937	-12.1888	-5.6972	17.886	1.98432	3.7429	378.88	3.7429	3.47775
LUMO	-0.06573								
B3LYP /6-311++G (d, p)									
HOMO	-0.20796	3.9119	-5.65888	1.7469	4.78364	7.40588	154.7860	7.40585	177.1691
LUMO	-0.06420								

4.7. Global and local reactivity descriptors

Based on the density functional descriptors, global chemical reactivity descriptors of title molecule such as global hardness (η), chemical potential (μ), global softness (σ), electronegativity (χ), ionization potential (I), electron affinity (A) and global electrophilicity (ω) as well as local reactivity have been defined [40,41] as follows:

$$\eta = \frac{1}{2}\left(\frac{\partial^2 E}{\partial N^2}\right)_{V(r)} = \frac{1}{2}\left(\frac{\partial \mu}{\partial N}\right)_{V(r)}$$

$$\mu = \left(\frac{\partial E}{\partial N}\right)_{V(r)}$$

$$\chi = -\mu = -\left(\frac{\partial E}{\partial N}\right)_{V(r)}$$

where E is the total energy, N is the number of electrons of the chemical species, η is the chemical potential and V(r) is the external potential, which is identified as the negative of the electronegativity (χ) as defined by Iczkowski and Margrave [42]. According to Koopman's theorem [43], the entries of the HOMO and the LUMO orbital's of the molecule are related to the ionization potential (I) and the electron affinity (A), respectively, by the following reactions:

$$I = -E_{HOMO}$$

$$A = -E_{LUMO}$$

Absolute electronegativity (χ) and absolute hardness (η) of the molecule are given by [59], respectively. Softness (σ) is a property of compared the measures the extent of chemical reactivity. It is the reciprocal of hardness.

$$\chi = (1 + A)/2$$

$$\eta = (1 - A)/2$$

$$\sigma = \frac{1}{\eta}$$

Recently Parr et al. [44] have defined a new descriptor to quantity of global electrophilic power of the compound as electrophilicity index (ω) in terms of chemical potential and hardness as follows:

$$\omega = \left(\frac{\mu^2}{2\eta}\right)$$

All the calculate values of quantum chemical parameters of the moleculre in both basis sets of DFT are presented in

CONCLUSION

In the present work, the optimized molecular structure of the stable conformer, vibrational and electronic properties of the title compound have been calculated by DFT method (B3LYP) using 6-31+G (d) basis set. The optimized geometric parameters (bond lengths and bond angles) are theoretically determined and compared with the experimental results. Spectroscopic properties of the present molecule were examined by FT-IR and FT-Raman techniques. The complete vibrational assignments of wavenumbers are made on the basis of potential energy distribution (PED). The electronic properties are also calculated in different solvent with UV-Vis spectrum. The energies of MOs and the λ_{max} of the compound are also evaluated TD-DFT/B3LYP method with 6-31+G (d) basis set. The calculated HOMO, LUMO energy and frontier orbital energy gap values along with study for better understanding of charge transfer occur within the molecule.

REFERENCES

[1] R.N. Griffin, *Photochem. Photobiol.* 7, 1968, 159−173.
[2] L. Lindqvist, *J. Phys. Chem.* 76, 1972, 821−822.
[3] X. Zhang, L. Shan, H. Huang, X. Yang, X. Liang, A. Xing, H. Huang, X. Liu, J. Su, W. Zhang, *J. Pharm. Biomed. Anal*. 49, 2009, 715–725.
[4] Z.B. Liu, Y.S. Sun, J.H. Wang, H.F. Zhu, H.Y. Zhou, J.N. Hu, J. Wang, *Sep. Purif. Technol*. 64, 2008, 247–252.
[5] Y.R. Prasad, A.S. Rao, R. Rambabu, *Asian J. Chem*. 21, 2009, 907–914.
[6] S. Cacchi, G. Fabrizi, F. Gavazza, A. Goggiamani, *Org. Lett*. 5, 2003, 289–291.
[7] P.M. Sivakumar, G. Sheshayan, M. Doble, *Chem. Biol. Drug Des*. 72, 2008, 303–313.
[8] H.Z. Wei, L.C. Wing, H.L. Yuan, S.S. Yau, C.L. Yong, H.Y. Chi, *Heterocycles*, 45, 1997, 71–75.
[9] M.J. Climent, A. Corma, S. Iborra, A. Velty, *J. Catal*. 221, 2004, 474–482.
[10] H.G. Korth, M.I. de Heer, P. Mulder, *J. Phys. Chem*. 106, 2002, 8779–8789.
[11] A. Asensio, N. Kobko, J.J. Dannenberg, *J. Phys. Chem. A* 107, 2003, 6441–6443.
[12] M.J. Frisch, et al., GAUSSIAN 09, Revision A. 9, Gaussian, INC, Pittsburgh, 2009.
[13] H.B. Schlegel, *J. Comput. Chem*. 3, 1982, 214−218.
[14] E.D. Glendening, A.E. Reed, J.E. Carpenter, F. Weinhold. NBO Version 3.1.TCI. University of Wisconsin, Madison, 1998.
[15] T. Sundius, *J. Mol. Struct*. 218, 1990, 321−326; MOLVIB: A Program for Harmonic force field calculations. QCPE Program No. 807, 2002.

[16] P.L. Polavarapu, *J. Phys. Chem.* 94, 1990, 8106−8112.
[17] G. Keresztury, BT Raman spectroscopy. Theory, in: J.M. Chalmers, P.R. Griffiths (Eds.), Handbook of Vibrational Spectroscopy, Vol. 1, John Wiley & Sons Ltd., 2002, 71−87.
[18] Uwe Monkowius, Manfred Zabel, *Acta Cryst Sec. E* 64, 2008, m196.
[19] Min Zhang, Xian-You Yuan, Seik Weng Ng, *Acta Cryst. Sec. E* 66, 2010, o2917.
[20] E.G. Lewars, computational chemistry, Spriger Science, Business media. B.V., 2011, doi: 10:1007/978−90-481-3862-3-2.
[21] N.P.G. Roges, A Guide to the Complete Interpretation of Infrared Spectra of Organic Structures, Wiley, New York, 1994.
[22] V. Krishnakumar, N. Surumbakuzhali, S. Muthunatesan, *Spectrochim. Acta A* 71, 2009, 1810–1813.
[23] G. Socrates, Infrared Characteristic Group Frequencies, John Wiley & Sons,Interscience Publication, New York, Brisbane, Toronto 1980
[24] G. Varsanyi, Assignments for Vibrational Spectra of Seven Hundred Benzene Derivatives, vol. 1/2, Academic Kiado, Budapset, 1973.
[25] S. Gunasekaran, R. ArunBalaji, S. Seshadri, S. Muthu, *Indian J. Pure Appl. Phys*. 46, 2008, 162–168.
[26] S.Saravanan, V. Balachandran, K. Viswanathan, *Spectrochim. Acta part A* 121, 2014, 685−697.

